

Perturbative Yukawa theory at finite density: the role of masses and renormalization group flow at two loops

Letícia F. PALHARES* and Eduardo S. FRAGA†
Instituto de Física, Universidade Federal do Rio de Janeiro
C.P. 68528, Rio de Janeiro, RJ 21941-972, Brazil

Yukawa theory at vanishing temperature provides (one of the ingredients for) an effective description of the thermodynamics of a variety of cold and dense fermionic systems. We study the role of masses and the renormalization group flow in the calculation of the equation of state up to two loops within the $\overline{\text{MS}}$ scheme. Two-loop integrals are computed analytically for *arbitrary* fermion and scalar masses, and expressed in terms of well-known special functions. The dependence of the renormalization group flow on the number of fermion flavors is also discussed.

I. INTRODUCTION

Cold and dense fermionic systems are found in a wide range of physical environments and energy scales. In condensed matter, for instance, in the phenomena of antiferromagnetic ordering and superconductivity in the Hubbard model [1]. Increasing dramatically the density, Fermi pressure is responsible for compensating gravity in the hydrostatic equilibrium of compact stars, the Fermi gas being formed by electrons, neutrons or even quarks, depending on the density and formation process [2]. In nuclear and particle physics, hadrons undergo chiral and deconfinement transitions at sufficiently large baryonic densities [3], exhibiting a very rich phenomenology including several color superconducting phases according to the different possibilities for quark pairing [4].

Unfortunately, the thermodynamics of such plasmas in the case of vanishing temperature and finite density is not very amenable to first-principle calculations. On one hand, the so-called *sign problem* brings about major technical difficulties for performing Monte Carlo lattice simulations at finite chemical potential [5]. On the other hand, although the perturbative series for the thermodynamic potential at zero temperature and finite density seems to be much better behaved than its counterpart at finite temperature [6, 7, 8, 9], the values of chemical potential that are phenomenologically interesting usually have some overlap with a region where the coupling becomes large due to renormalization group running, so that perturbative calculations break down. Therefore, one is usually compelled to resort to effective theories, either to simplify the original description in terms of a fundamental theory, but still keeping its relevant symmetries, or to complement a given perturbative approach in the region where the coupling becomes large.

In spite of the fact that an effective theory does not require renormalizability to be well posed, this attribute is highly desirable if one is interested in investigating the behavior of physical quantities as the energy scale is modified, as discussed above, which can be accomplished via renormalization group methods. The requirement of renormalizability restricts considerably the spectrum of possibilities, and in most cases the effective theory will contain a Yukawa sector. In fact, the Yukawa theory is very common in particle and nuclear physics, not only because it is very convenient in building effective models but also due to the need for a mechanism of spontaneous symmetry breaking and mass generation in gauge theories. In condensed matter systems exhibiting phase transitions, such as the antiferromagnetic-superconductor transition mentioned above, the situation is analogous. Thus, perturbative Yukawa theory in a medium has a wide range of applications. When it represents a sector of a fundamental theory, such as the quark-Higgs sector of the electroweak theory, one must assure that the scales are such that the Landau pole is not reached within the region of investigation, so that one can compute loop corrections and implement a renormalization group (RG) analysis. On the other hand, when it plays the role of part of an effective theory, one can avoid the Landau pole by simply introducing a cutoff beyond which the theory is meaningless. In the latter, one can choose to take effects from RG flow into account or not, depending on the system under investigation.

In either case, the perturbative treatment of the Yukawa theory at finite density may be of help also for testing lattice simulations in the limit of small coupling. In fact, numerical studies at zero temperature and density of the Yukawa theory with a real scalar field [10] and of the chirally invariant Higgs-Yukawa model [11] have revealed a rich structure, in spite of the formal simplicity of the theory. In some cases perturbative calculations may complement in an efficient way Monte Carlo simulations in the investigation of the phase structure of a given effective theory [12], in others the effective model can use lattice data as input for its parameters [13].

* leticia@if.ufrj.br

† fraga@if.ufrj.br

In this paper we investigate the role of masses and the RG flow in the calculation of the equation of state of cold and dense Yukawa theory up to two loops within the $\overline{\text{MS}}$ scheme. Previously we have presented preliminary results on the two-loop correction for the pressure with one massive fermion flavor and a massless scalar field [14] and the influence of the RG running on the equation of state for N_F flavors [15]. The interest in studying results for different numbers of flavors, such as $N_F = 4$, is motivated not only by the phenomenological interest in different physical systems but also by on-going studies on the lattice using Kogut-Susskind fermions [16]. Here we present full results for the thermodynamic potential with arbitrary masses and number of fermion species, including the effects from RG flow of couplings and masses. The two-loop momentum integrals are computed analytically for *arbitrary* fermion and scalar masses, the final result being expressed in terms of well-known special functions. Renormalization is implemented in the standard fashion in the $\overline{\text{MS}}$ scheme.

The paper is organized as follows. In Section II we show our results for the two-loop expansion of the thermodynamic potential of the Yukawa theory at finite density, and discuss the renormalization procedure. Fixed mass and coupling results are presented in Section III. In Section IV we study the coupling and mass RG flows and their influence on the pressure. Section V contains our conclusions and outlook. Several technical details are left for a final appendix.

II. TWO-LOOP THERMODYNAMIC POTENTIAL

In what follows, we consider a gas of N_F flavors of massive spin-1/2 fermions whose interaction is mediated by a massive real scalar field, ϕ , with an interaction term of the Yukawa type, so that the Lagrangian has the following general form:

$$\mathcal{L}_Y = \mathcal{L}_\psi + \mathcal{L}_\phi + \mathcal{L}_{int}, \quad (1)$$

where

$$\mathcal{L}_\psi = \sum_{\alpha=1}^{N_F} \bar{\psi}_\alpha (i\cancel{\partial} - m) \psi_\alpha, \quad (2)$$

$$\mathcal{L}_\phi = \frac{1}{2}(\partial_\mu \phi)(\partial^\mu \phi) - \frac{1}{2}m_\phi^2 \phi^2 - \lambda_3 \phi^3 - \lambda \phi^4, \quad (3)$$

$$\mathcal{L}_{int} = \sum_{\alpha=1}^{N_F} g \bar{\psi}_\alpha \psi_\alpha \phi. \quad (4)$$

Here, m and m_ϕ are the fermion and boson masses, respectively, assuming all the fermions have the same mass, for simplicity. The Yukawa coupling is represented by g ; λ_3 and λ are bosonic self-couplings allowed by renormalizability. The latter play no role in the thermodynamics up to this order, unless in the presence of a nonzero scalar condensate [17], as in the case of a spontaneously broken symmetry, where the condensate contributes to the effective masses. In this paper we assume $\langle \phi \rangle = 0$, leaving the treatment of spontaneous symmetry breaking, as in the linear sigma model, for a future publication [18].

Although we are interested in the limit in which the temperature T vanishes, it is technically more convenient to work with the imaginary time formalism of finite-temperature field theory, where the time dimension is compactified and associated with the inverse temperature $\beta = 1/T$ [19]. At the end, we shall take the limit $T \rightarrow 0$. As is well-known, to be consistent with the spin-statistics theorem for bosons (B) and fermions (F), one has to impose, respectively, the fields to be periodic or anti-periodic in the imaginary time τ , so that only specific discrete Fourier modes are allowed. Therefore, as is customary in finite-temperature field theory, integrals over the zeroth four-momentum component are replaced by discrete sums over Matsubara frequencies, denoted by $\omega_n^B = 2n\pi T$ and $\omega_n^F = (2n+1)\pi T$, with n integer. Taking finite density effects into account amounts to incorporating the constraint of conservation of the fermion number which, in practice, is implemented by a shift in the zeroth component of the fermionic four-momentum $p^0 = i\omega_n^F \mapsto p^0 = i\omega_n^F + \mu$, μ being the chemical potential.

From the partition function written in terms of the euclidean action for Eq. (1), $Z_Y(T, \mu) = \text{Tr} \exp(-S_Y)$, one derives the perturbative series for the thermodynamic potential $\Omega_Y \equiv -(1/\beta V) \ln Z_Y$:

$$\Omega_Y = -\frac{1}{\beta V} \ln Z_0 - \frac{1}{\beta V} \ln \left[1 + \sum_{\ell=1}^{\infty} \frac{(-1)^\ell}{\ell!} \langle S_{int}^\ell \rangle_0 \right], \quad (5)$$

where V is the volume of the system, Z_0 is the partition function of the free theory and S_{int} represents the euclidean interaction action. Notice that Wick's theorem implies that only even powers in the above expansion survive, yielding

a power series in $\alpha_Y \equiv g^2/4\pi$ [20]. Omitting purely bosonic contributions (which are μ -independent) and the diagrams representing counterterms, the thermodynamic potential up to two loops is given, diagrammatically, by

$$\Omega_Y = \frac{1}{\beta V} N_F \text{ (circle with solid lines) } + \frac{1}{2} \frac{1}{\beta V} N_F \text{ (circle with solid lines and dashed line) } + O(\alpha_Y^2), \quad (6)$$

where solid lines represent the fermions and dashed lines stand for the bosons. The first diagram corresponds to the free gas contribution [19]

$$\text{ (circle with solid lines) } = -2V \int \frac{d^3 \mathbf{p}}{(2\pi)^3} \left[\beta E_{\mathbf{p}} + \ln \left(1 + e^{-\beta(E_{\mathbf{p}} - \mu)} \right) + \ln \left(1 + e^{-\beta(E_{\mathbf{p}} + \mu)} \right) \right], \quad (7)$$

with $E_{\mathbf{p}} = (\mathbf{p}^2 + m^2)^{1/2}$. The zero-point energy divergent term can be absorbed by a convenient redefinition of the zero of the thermodynamic potential, since it is independent of T and μ . The $O(\alpha_Y)$ correction is given by the exchange term [19]:

$$\text{ (circle with solid lines and dashed line) } = \beta V g^2 \int \! \! \! \int_{P_1, P_2, K} \text{Tr} \left[\frac{(2\pi)^3 \beta \delta^{(4)}(K - P_1 + P_2)}{(\not{P}_1 - m)(m_\phi^2 - K^2)(\not{P}_2 - m)} \right], \quad (8)$$

where the trace is performed over the Dirac structure, and the 4-momenta are given in terms of the Matsubara frequencies and the 3-momenta for fermions, $P_i = (p_i^0 = i\omega_{n_i}^F + \mu, \mathbf{p}_i)$, and bosons, $K = (k^0 = i\omega_l^B, \mathbf{k})$. We use the metric tensor $g^{\mu\nu} = \text{diag}(+, -, -, -)$ and the following notation for the sum-integrals:

$$\int \! \! \! \int_P = T \sum_n \int \frac{d^3 \mathbf{p}}{(2\pi)^3}. \quad (9)$$

The calculation of the exchange diagram is very similar for different theories and is a standard exercise in finite-temperature field theory, the main difference in details coming from the tensor structure of each theory under investigation. Previous results for cold and dense systems can be found, for instance, in Ref. [21] for nuclear matter, in Refs. [22, 23, 24] for QED and in Refs. [24, 25, 26, 27, 28, 29] for QCD (see also Ref. [19]). After some long but straightforward algebra, we can write the exchange term for the Yukawa theory in the following form (see Appendix):

$$\begin{aligned} \text{ (circle with solid lines and dashed line) } &= \beta V g^2 \int \frac{d^3 \mathbf{p}_1 d^3 \mathbf{p}_2}{(2\pi)^6} \frac{1}{2\omega_{12} E_{\mathbf{p}_1} E_{\mathbf{p}_2}} \left\{ \overline{\mathcal{J}}_+ \omega_{12} \Sigma_1 + \overline{\mathcal{J}}_- \omega_{12} \Sigma_2 + \right. \\ &+ 2 \left[\overline{\mathcal{J}}_- E_+ - \overline{\mathcal{J}}_+ E_- \right] n_b(\omega_{12}) N_f(1) - \\ &- \left[\overline{\mathcal{J}}_+(E_- + \omega_{12}) - \overline{\mathcal{J}}_-(E_+ - \omega_{12}) \right] N_f(1) - \\ &- 2 \overline{\mathcal{J}}_- E_+ n_b(\omega_{12}) - \\ &\left. - \overline{\mathcal{J}}_-(E_+ - \omega_{12}) \right\}, \quad (10) \end{aligned}$$

where we have defined the following functions:

$$\overline{\mathcal{J}}_{\pm} \equiv -2 \frac{m^2 - \mathbf{p}_1 \cdot \mathbf{p}_2 \pm E_{\mathbf{p}_1} E_{\mathbf{p}_2}}{E_{\mp}^2 - \omega_{12}^2} = 1 - \frac{4m^2 - m_\phi^2}{E_{\mp}^2 - \omega_{12}^2}, \quad (11)$$

$$N_f(i) \equiv n_f(E_{\mathbf{p}_i} + \mu) + n_f(E_{\mathbf{p}_i} - \mu), \quad (12)$$

$$\Sigma_1 \equiv n_f(E_{\mathbf{p}_1} + \mu) n_f(E_{\mathbf{p}_2} + \mu) + n_f(E_{\mathbf{p}_1} - \mu) n_f(E_{\mathbf{p}_2} - \mu), \quad (13)$$

$$\Sigma_2 \equiv n_f(E_{\mathbf{p}_1} + \mu) n_f(E_{\mathbf{p}_2} - \mu) + n_f(E_{\mathbf{p}_1} - \mu) n_f(E_{\mathbf{p}_2} + \mu), \quad (14)$$

with $E_{\pm} \equiv E_{\mathbf{p}_1} \pm E_{\mathbf{p}_2}$ and $\omega_{12} \equiv \left(|\mathbf{p}_1 - \mathbf{p}_2|^2 + m_\phi^2 \right)^{1/2}$; $n_b(\omega) = [\exp(\beta\omega) - 1]^{-1}$ and $n_f(E) = [1 + \exp(\beta E)]^{-1}$ are the Bose-Einstein and the Fermi-Dirac distributions, respectively.

The physical meaning of each term in Eq. (10) is clear. The first two lines are quadratic in the statistic distributions, representing contributions coming from the scattering of particles from the medium. These are therefore ultraviolet finite due to the exponential suppression of the integrands implemented by the distributions. The other terms contain contributions coming from the scattering of virtual particles. The last term is a pure vacuum contribution, independent of T and μ , and can be absorbed by a redefinition of the zero of the thermodynamic potential. On the other hand, the remaining terms mix medium and vacuum particles, being linear in the statistic distributions, and call for renormalization.

The divergent contributions that are linear in n_b , \mathbf{L}_b , and linear in n_f , \mathbf{L}_f , can be written in terms of amputated (*amp*) vacuum (*vac*) self-energies evaluated on the mass shell (*m.s.*) as follows (see Appendix):

$$\mathbf{L}_f = -2 \beta V \left\{ \int_{\mathcal{F}_P}^f (-1) \text{Tr} \left[\frac{1}{\not{P} - m} \left(i \begin{array}{c} \text{---} \bullet \text{---} \text{---} \bullet \text{---} \\ \text{---} \text{---} \text{---} \text{---} \end{array} \begin{array}{c} \text{---} \text{---} \text{---} \text{---} \\ \text{---} \text{---} \text{---} \text{---} \end{array} \begin{array}{c} \text{---} \text{---} \text{---} \text{---} \\ \text{---} \text{---} \text{---} \text{---} \end{array} \end{array} \right) \begin{array}{c} \text{---} \text{---} \text{---} \text{---} \\ \text{---} \text{---} \text{---} \text{---} \end{array} \begin{array}{c} \text{---} \text{---} \text{---} \text{---} \\ \text{---} \text{---} \text{---} \text{---} \end{array} \end{array} \right] \begin{array}{c} \text{---} \text{---} \text{---} \text{---} \\ \text{---} \text{---} \text{---} \text{---} \end{array} \begin{array}{c} \text{---} \text{---} \text{---} \text{---} \\ \text{---} \text{---} \text{---} \text{---} \end{array} \end{array} \right\}_{\text{matter}}^{\text{vac}} \quad (15)$$

$$\mathbf{L}_b = -\frac{\beta V}{N_F} \left\{ \int_{\mathcal{F}_Q}^f \frac{1}{m_\phi^2 - Q^2} \left(i \begin{array}{c} \text{---} \text{---} \text{---} \text{---} \\ \text{---} \text{---} \text{---} \text{---} \end{array} \begin{array}{c} \text{---} \text{---} \text{---} \text{---} \\ \text{---} \text{---} \text{---} \text{---} \end{array} \begin{array}{c} \text{---} \text{---} \text{---} \text{---} \\ \text{---} \text{---} \text{---} \text{---} \end{array} \end{array} \right) \begin{array}{c} \text{---} \text{---} \text{---} \text{---} \\ \text{---} \text{---} \text{---} \text{---} \end{array} \begin{array}{c} \text{---} \text{---} \text{---} \text{---} \\ \text{---} \text{---} \text{---} \text{---} \end{array} \end{array} \right\}_{\text{matter}}^{\text{vac}} \quad (16)$$

Here, *matter* means that the pure vacuum part has already been subtracted, and, while $K = (\omega_{\mathbf{k}}, \mathbf{k})$ and $P_1 = (E_{\mathbf{p}_1}, \mathbf{p}_1)$ are evaluated on the mass shell, $Q = (i\omega_l^B, \mathbf{k})$ and $P = (i\omega_n^F + \mu, \mathbf{p}_1)$ are not. Implementing the renormalization procedure for the self-energies above in the $\overline{\text{MS}}$ scheme, one obtains the renormalized expressions (see Appendix)

$$\mathbf{L}_f^{\text{ren}} = -2 \beta V \frac{\alpha_Y}{4\pi} 4m^2 \int \frac{d^3 \mathbf{p}_1}{(2\pi)^3} \left[\frac{N_f(1)}{2E_{\mathbf{p}_1}} \right] [\alpha_1], \quad (17)$$

$$\mathbf{L}_b^{\text{ren}} = -2 \beta V \frac{\alpha_Y}{4\pi} \int \frac{d^3 \mathbf{k}}{(2\pi)^3} \left[\frac{2n_b(\omega_{\mathbf{k}})}{2\omega_{\mathbf{k}}} \right] [2\alpha_2 + 6\alpha_3], \quad (18)$$

where

$$\alpha_1 = -4 \frac{m_\phi}{m} \left(1 - \frac{m_\phi^2}{4m^2} \right)^{\frac{3}{2}} \left\{ \tan^{-1} \left[\sqrt{\frac{1}{\frac{4m^2}{m_\phi^2} - 1}} \right] + \tan^{-1} \left[\frac{\frac{1}{2} - \frac{m_\phi^2}{4m^2}}{\sqrt{\frac{m_\phi^2}{4m^2} \sqrt{1 - \frac{m_\phi^2}{4m^2}}}} \right] \right\} + \frac{7}{2} - \frac{m_\phi^2}{2m^2} - \frac{3}{2} \log \left(\frac{m^2}{\Lambda^2} \right) + \frac{m_\phi^2}{m^2} \left(\frac{3}{2} - \frac{m_\phi^2}{4m^2} \right) \log \left(\frac{m^2}{m_\phi^2} \right), \quad (19)$$

$$\alpha_2 = m^2 - \frac{1}{6} m_\phi^2, \quad (20)$$

$$\alpha_3 = \frac{2}{3} \left[2m^2 - \frac{5}{12} m_\phi^2 \right] - \frac{1}{3} m_\phi^2 \left(\frac{4m^2}{m_\phi^2} - 1 \right)^{\frac{3}{2}} \tan^{-1} \left[\frac{1}{\sqrt{\frac{4m^2}{m_\phi^2} - 1}} \right] - \left(m^2 - \frac{m_\phi^2}{6} \right) \log \left(\frac{m^2}{\Lambda^2} \right), \quad (21)$$

and Λ is the renormalization subtraction point.

In the limit of vanishing temperature and in the absence of a scalar condensate, the Bose-Einstein distribution vanishes, so that the purely bosonic diagrams, omitted in Eq. (6), do not contribute. The Fermi-Dirac distribution simplifies to the Heaviside step function, $\lim_{T \rightarrow 0} n_f(E_{\mathbf{p}} - \mu) = \theta(\mu - E_{\mathbf{p}})$, signaling the occupation of all states in the interior of the Fermi surface. Simplifying all the terms in the thermodynamic potential, we obtain in the cold and dense limit

$$\Omega_Y = -N_F \frac{1}{24\pi^2} [2\mu p_f^3 - 3m^2 u] - \frac{1}{2} N_F 4\pi\alpha_Y \left[J_1 + \frac{1}{16\pi^4} m^2 u \alpha_1 \right], \quad (22)$$

where $u \equiv \mu p_f - m^2 \log \left(\frac{\mu + p_f}{m} \right)$, p_f is the Fermi momentum $p_f \equiv \sqrt{\mu^2 - m^2}$ and we have defined the integral

$$J_1 \equiv - \int \frac{d^3 \mathbf{p}_1 d^3 \mathbf{p}_2}{(2\pi)^6} \frac{1}{2E_{\mathbf{p}_1} E_{\mathbf{p}_2}} \bar{\mathcal{J}}_+ \theta(\mu - E_{\mathbf{p}_1}) \theta(\mu - E_{\mathbf{p}_2}). \quad (23)$$

The evaluation of the integral above when both fields are massive is highly non-trivial, and results are usually presented in the limit of at least one vanishing mass, which is the proper case in gauge theories, or numerically [19]. We obtained the following complete analytic result for *arbitrary* values of m , m_ϕ and μ (see Appendix for details)

$$J_1 = \frac{1}{(2\pi)^4} \left\{ 2m^2 \left(1 - \frac{m_\phi^2}{4m^2} \right) \mathcal{I}_I - \frac{1}{2} u^2 \right\}, \quad (24)$$

where the function \mathcal{I}_I is given by

$$\begin{aligned} \mathcal{I}_I = & \mu^2 \frac{m_\phi^2}{2m^2} \log \left[\frac{m_\phi^2}{4p_f^2 + m_\phi^2} \right] + \left(1 - \frac{m_\phi^2}{2m^2} \right) \frac{u^2 - \mu^2 p_f^2}{m^2} + \\ & + \frac{m_\phi}{m} \sqrt{1 - \frac{m_\phi^2}{4m^2}} (\mu p_f + u) D_{\tan} + p_f^2 - 2m^2 \bar{\mathcal{K}}_{\log} \left(\frac{p_f}{\mu + m}, \frac{m_\phi^2}{4m^2} \right), \end{aligned} \quad (25)$$

with

$$D_{\tan} \equiv \tan^{-1} \left(\frac{-p_f m_\phi}{2m(\mu + m) \sqrt{1 - \frac{m_\phi^2}{4m^2}}} \right) + \tan^{-1} \left(\frac{p_f}{m_\phi \sqrt{1 - \frac{m_\phi^2}{4m^2}}} \left[2 - \frac{m_\phi^2}{2m(\mu + m)} \right] \right). \quad (26)$$

For $\bar{x} \equiv p_f/(\mu + m) < 1$ and $z \equiv m_\phi^2/4m^2$, we can write the function $\bar{\mathcal{K}}_{\log}(\bar{x}, z)$ as

$$\bar{\mathcal{K}}_{\log}(\bar{x}, z) = \sqrt{z} \Delta(\bar{x}, z) + \frac{1}{2} \sqrt{z(z-1)} \mathcal{C}_{\text{Li}}(\bar{x}, z), \quad (27)$$

where

$$\begin{aligned} \mathcal{C}_{\text{Li}}(\bar{x}, z) = & \left[\mathbf{Li}_2 \left(1 - (z - \sqrt{z(z-1)}) (1 - \bar{x}) \right) - \mathbf{Li}_2 \left(1 - (z + \sqrt{z(z-1)}) (1 - \bar{x}) \right) + \right. \\ & \left. + \mathbf{Li}_2 \left(\frac{1 - \bar{x}}{1 + \bar{x}} \left[1 - (z + \sqrt{z(z-1)}) (1 - \bar{x}) \right] \right) - \mathbf{Li}_2 \left(\frac{1 - \bar{x}}{1 + \bar{x}} \left[1 - (z - \sqrt{z(z-1)}) (1 - \bar{x}) \right] \right) \right] + \left[\bar{x} \mapsto -\bar{x} \right], \end{aligned} \quad (28)$$

with the Dilogarithm Function [30] defined as $\mathbf{Li}_2(z) \equiv \sum_{n=1}^{\infty} (z^n/n^2)$. The quantity Δ is defined in two regions, according to the ratio z , as

$$\Delta(\bar{x}, z) = \begin{cases} \Delta_{<}(\bar{x}, z) & , \text{ if } z < 1 \\ \Delta_{>}(\bar{x}, z) & , \text{ if } z > 1 \end{cases}, \quad (29)$$

where

$$\begin{aligned} \Delta_{<}(\bar{x}, z) = & \sqrt{1-z} \left\{ \log(1-\bar{x}) \left[\tan^{-1} \left(\frac{\sqrt{1-z}}{\sqrt{z}} \right) - \tan^{-1} \left(\frac{\sqrt{z(1-z)}}{z + \left(\frac{1+\bar{x}^2}{2\bar{x}} - 1 \right)^{-1}} \right) \right] + \right. \\ & \left. + \log(1+\bar{x}) \left[\tan^{-1} \left(\frac{\sqrt{1-z}}{\sqrt{z}} \right) - \tan^{-1} \left(\frac{\sqrt{z(1-z)}}{z + \left(\frac{1+\bar{x}^2}{2\bar{x}} + 1 \right)^{-1}} \right) - \pi \left[1 - \theta \left(mz \frac{(1+\bar{x})^2}{1-\bar{x}^2} - \frac{2m\bar{x}}{1-\bar{x}^2} \right) \right] \right] \right\}, \quad (30) \\ \Delta_{>}(\bar{x}, z) = & \frac{1}{2} \sqrt{z-1} \left\{ \log \left(\frac{1-\bar{x}^2}{(1+\bar{x})^2} \right) \log \left(\frac{|\sqrt{z}(1+\bar{x}^2) - 2\bar{x}\sqrt{z-1}|}{|\sqrt{z}(1+\bar{x}^2) + 2\bar{x}\sqrt{z-1}|} \right) + \right. \\ & + \pi^2 \left[-\theta[z(1-\bar{x}^2) - 1] - \theta \left(1 + \frac{\bar{x}}{(1-\bar{x}^2)\sqrt{z(z-1)}} [2 - z(1-\bar{x}^2)] \right) \right] + \\ & \left. + \theta \left(1 - \frac{\bar{x}}{(1-\bar{x}^2)\sqrt{z(z-1)}} [2 - z(1-\bar{x}^2)] \right) + 1 \right\}. \end{aligned} \quad (31)$$

With this general result for the thermodynamic potential for the cold and dense Yukawa theory, we can analyze the effects from the different nonzero masses and their competition, the role of the interaction and the renormalization scale, as well as the influence of the RG flow of the coupling and masses.

III. RESULTS AT A FIXED ENERGY SCALE

Let us start our study by the simpler case with fixed energy scale Λ . In practice, one can choose an appropriate value for Λ , in this case a parameter in a given effective theory, by imposing, e.g., known experimental constraints for the system under consideration. In the next section, we investigate the role played by Λ as the running scale in the RG flow of g , m and m_ϕ . For fixed Λ , the main issue is the influence of the masses which we illustrate separating the analysis into two cases, the first with $m_\phi = 0$, and then the general one.

A. Massless boson

When $m_\phi = 0$, the integrals involved in the computation of the thermodynamic potential at finite density simplify dramatically. In fact, the former complicated functions α_1 and J_1 reduce to

$$\lim_{m_\phi \rightarrow 0} \alpha_1 = \frac{7}{2} - \frac{3}{2} \log \left(\frac{m^2}{\Lambda^2} \right), \quad (32)$$

$$\lim_{m_\phi \rightarrow 0} J_1 = \frac{1}{32\pi^4} \{3 u^2 - 4 p_f^4\}, \quad (33)$$

so that the thermodynamic potential assumes the much simpler form

$$\Omega_Y = -N_F \frac{1}{24\pi^2} [2 \mu p_f^3 - 3m^2 u] - N_F \frac{\alpha_Y}{16\pi^3} \left\{ 3 u^2 - 4 p_f^4 + m^2 u \left[7 - 3 \log \left(\frac{m^2}{\Lambda^2} \right) \right] \right\}. \quad (34)$$

It is interesting to notice that the inclusion of mass for the fermions brings the presence of logarithmic corrections one order down in α_Y . This is a general feature, also manifest in theories such as QCD. In massless QCD, for instance, one has $\sim \alpha_s$ corrections at two loops and $\sim \{\alpha_s^2, \alpha_s^2 \log \alpha_s, \alpha_s^2 \log(\Lambda/\mu)\}$ at three loops [6, 7]. However, in the massive case one finds not only $\sim \alpha_s$ terms, but also a contribution $\sim m^2 \alpha_s \log(\Lambda/m)$ at two loops [29], analogous to the one that can be seen above. In our case, this feature will be important when we incorporate the RG running of α_Y and m . On the other hand, since the explicit dependence on Λ is logarithmic, the effect of its variation without the RG flow does not affect significantly the pressure [14] unless for very large values of the coupling, where perturbation theory is meaningless.

Figs. 1 and 2 illustrate, respectively, interaction and fermion mass effects on the two-loop pressure, $P = -\Omega_Y$, as a function of the chemical potential μ in units of the reference scale $\Lambda = \Lambda_{\overline{\text{MS}}}$. Fig. 1 shows that the pressure is raised as the system considered interacts more strongly, reaching a variation of $\sim 50\%$ in comparison with the free case for $\alpha_Y \approx 0.72$ and $(\mu - m) = 0.1 \Lambda_{\overline{\text{MS}}}$. This behavior observed at small chemical potentials is not maintained at large scales: there is a crossing at $(\mu - m) \approx 0.25 \Lambda_{\overline{\text{MS}}}$ so that the interaction effects tend to reduce the pressure of highly dense media, although the corrections in this regime appear to be less significant ($\lesssim 20\%$). In fact, since the Yukawa coupling is treated perturbatively, it is quite reasonable that interaction effects do not modify drastically the thermodynamics within the domain of validity of our calculations. Nevertheless, depending on the specificities of the system under investigation, corrections of a few percent as the ones obtained above may have impact on physical predictions.

On the other hand, the fermion mass is not linked directly to the expansion parameter and its effects are therefore not expected to be constrained by the perturbative framework. Indeed, Fig. 2 shows that the influence of finite fermion masses on the thermodynamics can be sensibly more consequential: at $\mu = 0.6 \Lambda_{\overline{\text{MS}}}$, for instance, the inclusion of fermions with mass $m = 0.4 \Lambda_{\overline{\text{MS}}}$ lowers the pressure by a factor of $\sim 1/5$ in comparison with the massless case. Even for masses one order of magnitude smaller than the reference scale $\Lambda_{\overline{\text{MS}}}$, the corrections are sizable for sufficiently small chemical potentials. Therefore, finite fermion masses alter significantly the thermodynamics of the Yukawa theory in a wide range of the parameter space and approximations that neglect them should be implemented cautiously.

This result represents another indication of the potential importance of fermion mass effects. Recently, the modifications brought about by finite masses have received increasing attention in different contexts, either because they have been underestimated before or due to the interest in high-precision tests, in experiments and in more realistic lattice simulations. In calculations within the Standard Model, for instance, there is a whole literature on multi-loop integrals that is progressively turning its attention to the inclusion of contributions due to non-vanishing fermion masses [31]. In QCD it was also pointed out recently that finite quark masses, especially the strange quark mass that

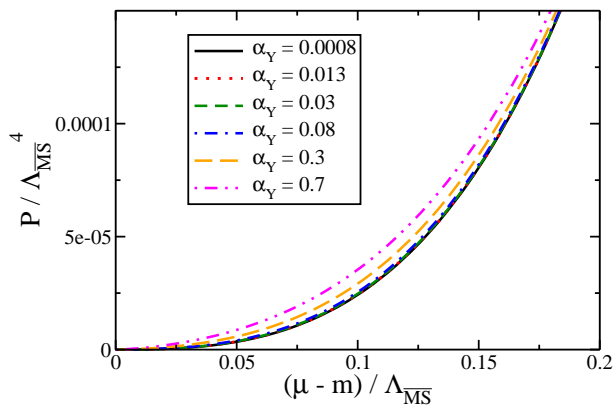


FIG. 1: Pressure normalized by the scale $\Lambda = \Lambda_{\overline{\text{MS}}}$ as a function of the fermion chemical potential for different values of the coupling g . The fermion mass is fixed at $m = 0.1\Lambda_{\overline{\text{MS}}}$.

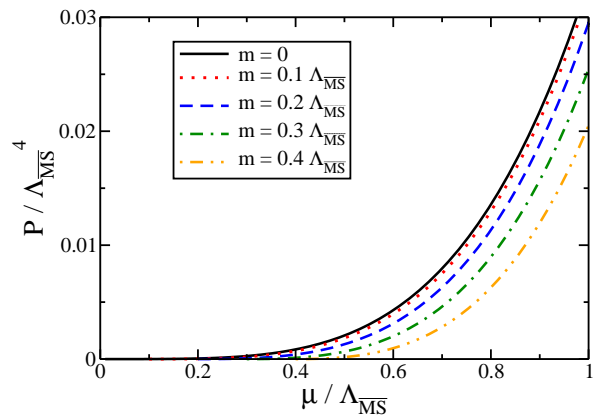


FIG. 2: Pressure normalized by the scale $\Lambda = \Lambda_{\overline{\text{MS}}}$ as a function of the fermion chemical potential for different values of the fermion mass m . The coupling is fixed at $\alpha_Y = 1/4\pi$.

is not that small compared to typical scales in QCD, should play an important role in the critical region of the chiral and the deconfining phase transitions [3], possibly bringing relevant astrophysical consequences [29]. These results for the Yukawa theory signal that also within effective theories mass effects bring relevant corrections.

B. General Case

Let us now consider the full massive case. The influence of the boson mass m_ϕ on the thermodynamics of the Yukawa theory is shown in Fig. 3. Since we are analyzing the cold and dense regime, the pressure investigated consists essentially in a quantum Fermi pressure. In this vein, it is convenient to interpret the results in terms of a free quasi-particle theory: the variation of the pressure can be seen as a consequence of the modification of the effective mass of the quanta present in the system through the radiative corrections to the fermionic self-energy due to the coupling with the bosons. We showed above, in Fig. 2, that for a given chemical potential the pressure for a theory of heavy fermions is lower than the one for light fermions. Therefore, Fig. 3 indicates that for m_ϕ/m sufficiently small the self-energy is negative, diminishing the fermionic effective mass and increasing the pressure. For the case illustrated in Fig. 3, this effect is inverted for $m_\phi/m \approx 15$. As one raises the chemical potential this behavior is intensified, as shown in Fig. 4.

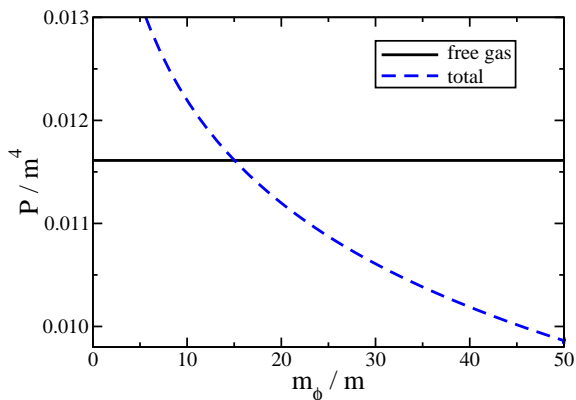


FIG. 3: Pressure normalized by the fermion mass m as a function of the ratio m_ϕ/m for $\mu = 4m/3$ and $\Lambda = 10m$.

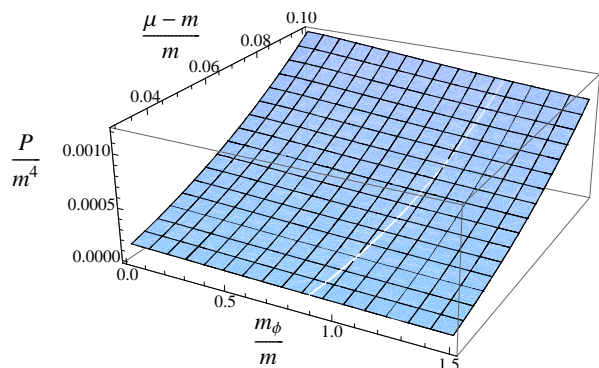


FIG. 4: Pressure normalized by the fermion mass m as a function of the ratio m_ϕ/m and μ ($\Lambda = 10m$).

However, it is important to stress that, from a quantitative point of view, these results depend strongly on the

renormalization scale Λ adopted. Although when analyzing a general theory it is not possible to discuss quantitatively the result, in the description of a specific system the renormalization scale is determined through physical constraints, such as positivity of the energy density and the domain of energies being investigated. In the case of QCD [6], for example, it is not reasonable for quark matter to have a higher pressure than a hadron gas for low chemical potentials (i.e., equivalent to densities of the order of the nuclear saturation density, $n_0 \approx 0.16 \text{ fm}^{-3}$), since this would imply the existence of stable deconfined matter in a density regime where only hadrons and nuclei are observed. Equivalently, one expects the quark pressure to be higher than the hadronic one for densities $n \gg n_0$. In this way, one fixes a physically reasonable range for the renormalization scale in QCD. This kind of procedure can also be implemented once the phenomenology described by an effective theory containing a Yukawa sector is known, and the parameters are given by experimental observations. Therefore, once the physical picture is fixed, the predictions above can be precised quantitatively.

IV. RG RUNNING EFFECTS

The thermodynamic potential Ω_Y depends on the renormalization scale Λ not only explicitly but also implicitly, through the RG running of the coupling and the masses, with Λ corresponding to typical momenta involved in scattering processes in the medium [32]. In the context of effective field theories, it is plausible to use the results above, with fixed α_Y and masses, and Λ determined by phenomenological constraints. Nevertheless, for several applications, RG flow may be considered a relevant feature or even be intrinsically present, as in the case of sectors of the Standard Model. Then, one has to solve the corresponding RG equations and include their effects in the evaluation of the equation of state. In fact, these effects bring major consequences in cold and dense QCD [6, 29]. Since we consider the general case of massive fermions and massive bosons, there will be an intricate competition between the different effects.

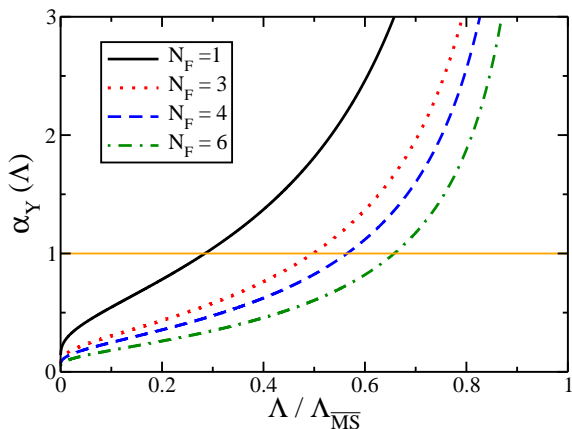


FIG. 5: Yukawa coupling RG flow normalized by the reference scale $\Lambda_{\overline{\text{MS}}}$ for different numbers of fermion flavors.

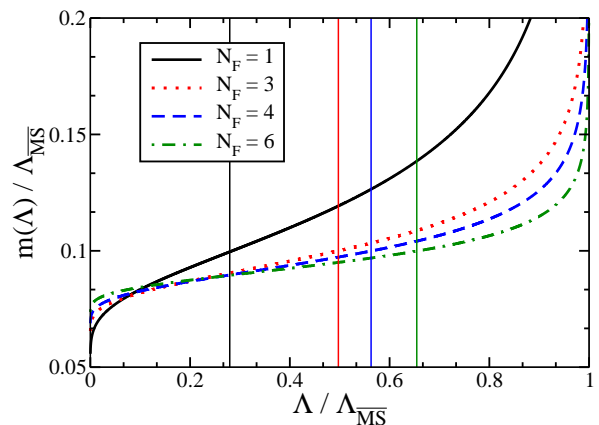


FIG. 6: Fermion mass RG flow normalized by the reference scale $\Lambda_{\overline{\text{MS}}}$ for different numbers of fermion flavors. We chose $m_0 = 0.1\Lambda_{\overline{\text{MS}}}$, and vertical lines represent the scale at which $\alpha_Y = 1$ for each value of N_F , increasing from left to right.

In what follows we include the effects from running masses and coupling, and also investigate the role of the number of fermion flavors N_F . Although we study the behavior of RG running for different numbers of flavors, our results for the pressure are presented for $N_F = 4$. This is motivated by on-going studies on the lattice using Kogut-Susskind fermions [16].

The running coupling of the Yukawa theory up to $O(\alpha_Y)$ was computed long ago [34] and reads

$$\alpha_Y(\Lambda) = \frac{1}{\frac{3+2N_F}{2\pi} \log\left(\Lambda_{\overline{\text{MS}}}/\Lambda\right)}. \quad (35)$$

Fig. 5 displays the scale dependence of the Yukawa coupling for different numbers of flavors. This plot illustrates the crucial role of N_F in the intensity of the interaction as a function of the energy scale and, therefore, in the delimitation

of the domain of validity of perturbative calculations. Raising N_F from 1 to 6, the energy scale at which the Yukawa coupling reaches one increases from $\sim 30\%$ to $\sim 70\%$ of the maximum scale $\Lambda_{\overline{\text{MS}}}$, a very significant effect. This is also clear from Eq. (35), where $\alpha_Y \sim 1/N_F$, which strongly suggests that a large N_F approach could be appropriate for theories with Yukawa-type couplings as has been noticed long ago in a different context by Gross and Neveu [35], who also identified the need to go beyond the large N_F expansion in order to obtain sensible results (see also [12]).

The fermion mass runs according to [15]

$$m(\Lambda) = [\alpha_Y(\Lambda)]^{\frac{3}{2(2N_F+3)}} m_0, \quad (36)$$

where m_0 is the value of the mass at the scale where $\alpha_Y = 1$, i.e.,

$$m_0 = m(\Lambda_0) \quad ; \quad \alpha_Y(\Lambda_0) = 1. \quad (37)$$

The RG flow of the fermion mass is plotted in Fig. 6. Once again, the number of flavors plays an important quantitative role. More interesting, though, is the following feature: in the large N_F limit fermion masses tend to become scale invariant, i.e., for larger values of N_F the running of m becomes flatter. In fact, from Eq. (36), the $N_F \rightarrow \infty$ behavior of $m(\Lambda)$ is $\sim [(1/N_F) \log(\Lambda_0/\Lambda)]^{1/N_F} m_0$, rendering RG corrections to m negligible very fast as N_F increases.

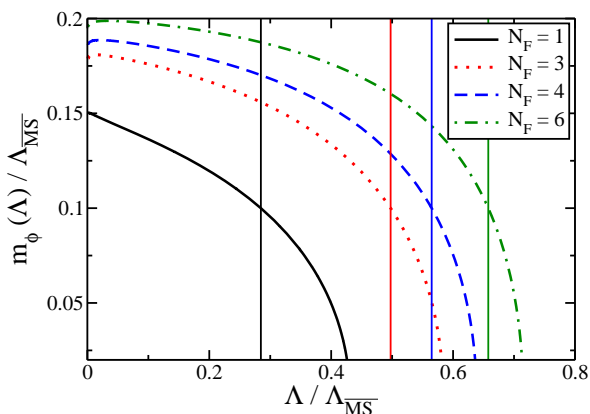


FIG. 7: Boson mass RG flow normalized by the reference scale $\Lambda_{\overline{\text{MS}}}$ for different numbers of fermion flavors for $m_0 = 0.1\Lambda_{\overline{\text{MS}}}$ and $m_{\phi,0} = 0.1\Lambda_{\overline{\text{MS}}}$.

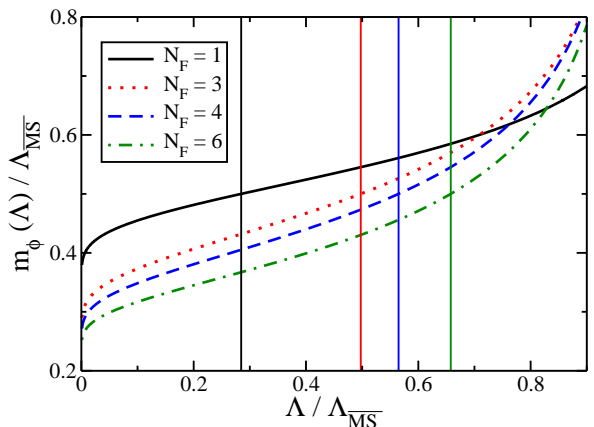


FIG. 8: Boson mass RG flow normalized by the reference scale $\Lambda_{\overline{\text{MS}}}$ for different numbers of fermion flavors for $m_0 = 0.1\Lambda_{\overline{\text{MS}}}$ and $m_{\phi,0} = 0.5\Lambda_{\overline{\text{MS}}}$.

The scale dependence of the effective mass of the bosonic field is determined by the following flow equation

$$\frac{\partial m_\phi^2}{\partial \log(\Lambda/\Lambda_{\overline{\text{MS}}})} = \alpha_Y \frac{N_F}{\pi} [m_\phi^2 - 6m^2], \quad (38)$$

with $\alpha_Y = \alpha_Y(\Lambda)$ and $m = m(\Lambda)$ given by (35) and (36), respectively. The solution of this equation can be written in the following form:

$$m_\phi^2(\Lambda) = m^2(\Lambda) \left\{ \frac{12N_F}{2N_F+3} + \mathcal{C} \left[\log\left(\frac{\Lambda}{\Lambda_{\overline{\text{MS}}}}\right) \right]^{-\frac{2N_F-3}{2N_F+3}} \right\}, \quad (39)$$

where \mathcal{C} is a constant fixed by the boundary condition $m_\phi(\Lambda_0) = m_{\phi,0}$, and is given by

$$\mathcal{C} = \left[\log\left(\frac{\Lambda_0}{\Lambda_{\overline{\text{MS}}}}\right) \right]^{\frac{2N_F-3}{2N_F+3}} \left\{ \frac{m_{\phi,0}^2}{m_0^2} - \frac{12N_F}{2N_F-3} \right\}. \quad (40)$$

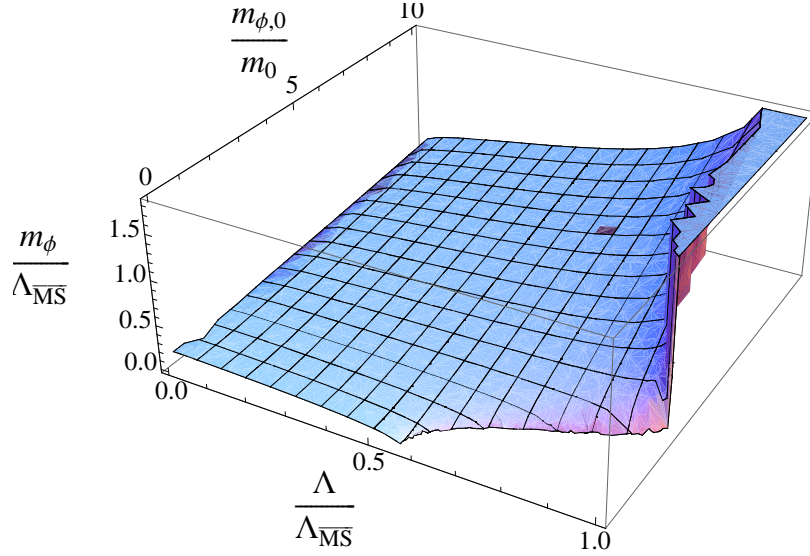


FIG. 9: Running boson mass as a function of Λ and the ratio of initial conditions $m_{\phi,0}/m_0$ in units of $\Lambda_{\overline{\text{MS}}}$.

It is clear from Eq. (38) that the RG flow for m_ϕ exhibits two possible regimes, allowing the boson effective mass to increase or to decrease depending on the sign of the term inside the brackets. We illustrate these cases in Fig. 7 and Fig. 8 for different numbers of fermion flavors. We also show the interpolation between these two regimes in a three-dimensional plot, Fig. 9, as we vary the boundary conditions $m_{\phi,0}/m_0$ for $N_F = 4$. For large values of N_F , the boson mass is strongly modified (either increasing or decreasing smoothly, depending on the regime), and the RG flow does not seem to become negligible in either case.

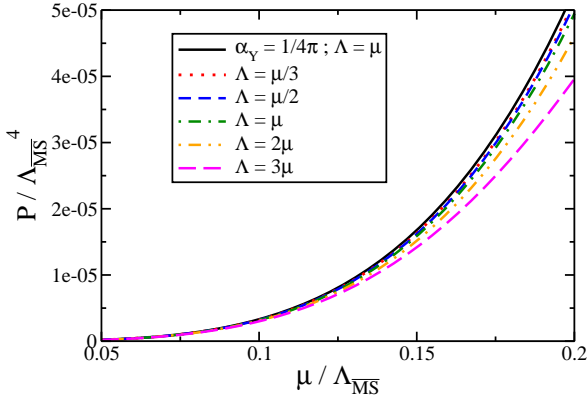


FIG. 10: Pressure versus chemical potential in units of the reference scale $\Lambda_{\overline{\text{MS}}}$ for $N_F = 4$ for different values of Λ/μ in the running of α_Y . Here, $m = 0$ and $m_\phi = 0$.

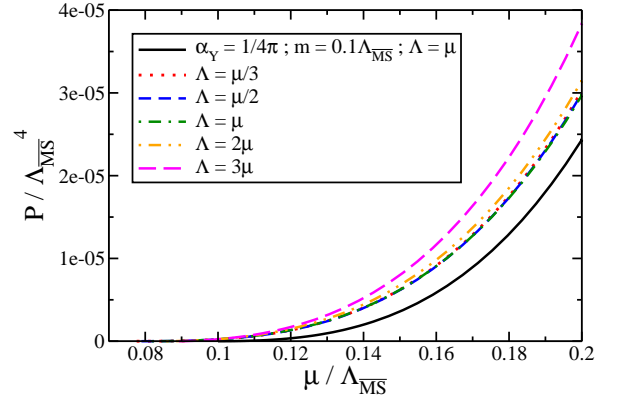


FIG. 11: Pressure versus chemical potential in units of the reference scale $\Lambda_{\overline{\text{MS}}}$ for $N_F = 4$ for different values of Λ/μ in the running of α_Y and m . Here, $m_\phi = 0$ and $m_0 = 0.1\Lambda_{\overline{\text{MS}}}$.

Since we consider a general Yukawa theory at finite density, the free parameters are arbitrary and allow for a wide spectrum of possibilities for the influence of the RG flow on the equation of state. So, although the RG flow is completely well defined by the results presented above, there still remains some freedom in the choice of the following scales: Λ , Λ_0 , m_0 and $m_{\phi,0}$. The first usually represents the typical scattering energy scale, and its behavior should be motivated physically. In the case of cold and dense matter, the customary natural guess is simply $\Lambda \sim \mu$, the range of reasonable values for the proportionality constant being determined by physical consistency of the effective theory. The others must be fixed by measured observables. Therefore, all of them depend on the specificities of the system under consideration. In a given physical system, these parameters can be determined by phenomenological constraints, as discussed above, and no ambiguity is left. In the general theory we consider, which describes a whole

class of possible physical systems, one can only exemplify the effects of the RG running by choosing a few illustrative cases.

RG flow effects on the pressure are displayed in Figs. 10 and 11 for certain choices of the free parameters, and for $N_F = 4$. To simplify the analysis, we opted to keep the bosons massless. In Fig. 10, we show the pressure for different values of Λ/μ for massless fermions. It is clear that the pressure is lowered as one increases Λ/μ . In the case of massive fermions, displayed in Fig. 11, the effect of the RG flow is exactly the opposite. This apparent contradiction is not surprising. It is actually a natural consequence of the major influence of the fermion mass on the pressure. The fact that the curve with fixed mass $m = 0.1\Lambda_{\overline{\text{MS}}}$ is much lower than the rest is just an artifact of our choice of fixed mass being much bigger than the effective mass for these densities.

V. CONCLUSIONS AND OUTLOOK

Yukawa theory at vanishing temperature provides at least one of the ingredients for an effective description of the thermodynamics of a variety of cold and dense fermionic systems, from condensed matter to particle physics. In this paper we have calculated the thermodynamic potential for a general Yukawa theory up to two loops within the $\overline{\text{MS}}$ scheme. We have explicitly considered the effect of *arbitrary* masses for both fields, the spinorial and the scalar, which renders the evaluation of two-loop integrals highly non-trivial. Nevertheless, all integrals were computed analytically and expressed in terms of well-known special functions. These results were verified against numerical results in several different regions of the parameter space. The role of RG running of coupling and masses was also investigated, as well as its dependence on the number of fermion flavors.

Our results show that the pressure is clearly lowered by increasing the mass of the fermions, this effect being much more relevant than the ones brought about by variations of the coupling. The effect of the scalar mass is also significant, and can be viewed, in a quasi-particle picture, as providing important corrections to the fermion mass which, as seen, modifies appreciably the equation of state. The role of the RG flow, on the other hand, is more fuzzy in the case of an arbitrary Yukawa theory, and our findings for its influence on the pressure were illustrated in a few representative cases. Once the physical system is specified, though, these ambiguities are completely resolved.

The behavior of running effects with increasing N_F is also quite interesting for two reasons. First, it is rather convenient for perturbative purposes since α_Y remains smaller than one even for higher values of the energy scale. Then, one could, for instance, compare lattice results to perturbative calculations in a wider range of energy scale. Second, because the flow of the fermion mass tends to flatten out, becoming much simpler. Thus, our equation of state in the case of $N_F = 4$ can be useful, for instance, in on-going studies on the lattice using Kogut-Susskind fermions [16] to deal with effective theories at finite density in the hope of bringing some understanding to the study of the Sign Problem [36].

To study the phase structure of systems such as the antiferromagnetic/superconductor in the Hubbard model [1], condensates in the core of neutron stars [2], and QCD, among many others, one has to generalize our description and include the presence of a non-zero condensate by computing the full effective potential. This calculation is under way for the linear sigma model, and will be presented elsewhere [18].

Acknowledgments

The authors thank D. Rischke, J. Schaffner-Bielich, and A. Taurines for fruitful discussions. This work was partially supported by CAPES, CNPq, FAPERJ and FUJB/UFRJ.

APPENDIX: IN-MEDIUM EXCHANGE DIAGRAM WITH MASSIVE FIELDS

In this appendix we discuss some technical details concerning the explicit calculation of the in-medium exchange contribution to the thermodynamic potential with both fermionic and bosonic non-zero masses.

1. Matsubara sums

From Eq. (8), solving the trace over Dirac indices and using the following representation of the Kronecker delta [26]:

$$\beta\delta_{n_1, n_2+l} = \frac{e^{\beta[k^0+p_2^0-\mu]} - e^{\beta[p_1^0-\mu]}}{p_1^0 - p_2^0 - k^0}, \quad (\text{A.1})$$

one obtains

$$\begin{array}{c} \text{---} \circ \text{---} \\ \text{---} \circ \text{---} \end{array} = \beta V g^2 \int \frac{d^3\mathbf{p}_1 d^3\mathbf{p}_2 d^3\mathbf{k}}{(2\pi)^6} \delta^{(3)}(\mathbf{k} - \mathbf{p}_1 + \mathbf{p}_2) \mathcal{S}(\mathbf{p}_1, \mathbf{p}_2, \mathbf{k}), \quad (\text{A.2})$$

where

$$\mathcal{S}(\mathbf{p}_1, \mathbf{p}_2, \mathbf{k}) = T \sum_l T \sum_{n_1} T \sum_{n_2} \frac{s_0(p_1^0, p_2^0, k^0)}{(P_1^2 - m^2)(m_\phi^2 - K^2)(P_2^2 - m^2)}, \quad (\text{A.3})$$

$$s_0(p_1^0, p_2^0, k^0) = \frac{4(P_1 \cdot P_2 + m^2)}{p_1^0 - p_2^0 - k^0} \left\{ \frac{1}{n_f(p_2^0 - \mu) n_b(k^0)} - \frac{1}{n_b(k^0)} + \frac{1}{n_f(p_2^0 - \mu)} - \frac{1}{n_f(p_1^0 - \mu)} \right\}. \quad (\text{A.4})$$

Resorting to the standard results

$$T \sum_l \frac{g(k^0)}{m_\phi^2 - K^2} = \frac{1}{2\omega} \{g(k^0) n_b(k^0)\}_{k^0=-\omega}^{k^0=\omega}, \quad (\text{A.5})$$

$$T \sum_n \frac{g(p^0)}{P^2 - m^2} = \frac{1}{2E_{\mathbf{p}}} \{g(p^0) n_f(p^0 - \mu)\}_{p^0=-E_{\mathbf{p}}}^{p^0=E_{\mathbf{p}}}, \quad (\text{A.6})$$

for the bosonic and fermionic Matsubara sums, respectively, with $g(q)$ an analytic function, the triple sum \mathcal{S} reads:

$$\begin{aligned} \mathcal{S}(\mathbf{p}_1, \mathbf{p}_2, \mathbf{k}) = & \frac{1}{8\omega E_{\mathbf{p}_1} E_{\mathbf{p}_2}} \left\{ \frac{4(P_1 \cdot P_2 + m^2)}{p_1^0 - p_2^0 - k^0} \left[n_f(p_1^0 - \mu) - n_f(p_1^0 - \mu) n_f(p_2^0 - \mu) + \right. \right. \\ & \left. \left. + n_f(p_1^0 - \mu) n_b(k^0) - n_f(p_2^0 - \mu) n_b(k^0) \right] \right\} \left| \begin{array}{l} p_1^0 = E_{\mathbf{p}_1} \\ p_1^0 = -E_{\mathbf{p}_1} \end{array} \right| \left| \begin{array}{l} p_2^0 = E_{\mathbf{p}_2} \\ p_2^0 = -E_{\mathbf{p}_2} \end{array} \right| \left| \begin{array}{l} k^0 = \omega \\ k^0 = -\omega \end{array} \right|. \quad (\text{A.7}) \end{aligned}$$

After a straightforward algebraic manipulation using the properties of the Fermi-Dirac and Bose-Einstein distributions, the above equation can be written as

$$\begin{aligned} \mathcal{S}(\mathbf{p}_1, \mathbf{p}_2, \mathbf{k}) = & 4 \frac{1}{8\omega E_{\mathbf{p}_1} E_{\mathbf{p}_2}} \left\{ (m^2 - \mathbf{p}_1 \cdot \mathbf{p}_2 + E_{\mathbf{p}_1} E_{\mathbf{p}_2}) \left[\frac{-2\omega}{E_-^2 - \omega^2} \right] \Sigma_1 + \right. \\ & + (m^2 - \mathbf{p}_1 \cdot \mathbf{p}_2 - E_{\mathbf{p}_1} E_{\mathbf{p}_2}) \left[\frac{2\omega}{-E_+^2 + \omega^2} \right] \Sigma_2 + \\ & + (m^2 - \mathbf{p}_1 \cdot \mathbf{p}_2 + E_{\mathbf{p}_1} E_{\mathbf{p}_2}) \left[\frac{2E_-}{E_-^2 - \omega^2} \right] n_b(\omega) [N_f(1) - N_f(2)] + \\ & + (m^2 - \mathbf{p}_1 \cdot \mathbf{p}_2 - E_{\mathbf{p}_1} E_{\mathbf{p}_2}) \left[\frac{-2E_+}{E_+^2 - \omega^2} \right] n_b(\omega) [N_f(1) + N_f(2)] + \\ & + \left[\frac{m^2 - \mathbf{p}_1 \cdot \mathbf{p}_2 + E_{\mathbf{p}_1} E_{\mathbf{p}_2}}{E_- - \omega} - \frac{m^2 - \mathbf{p}_1 \cdot \mathbf{p}_2 - E_{\mathbf{p}_1} E_{\mathbf{p}_2}}{E_+ + \omega} \right] N_f(1) - \\ & - \left[\frac{m^2 - \mathbf{p}_1 \cdot \mathbf{p}_2 + E_{\mathbf{p}_1} E_{\mathbf{p}_2}}{E_- + \omega} + \frac{m^2 - \mathbf{p}_1 \cdot \mathbf{p}_2 - E_{\mathbf{p}_1} E_{\mathbf{p}_2}}{E_+ + \omega} \right] N_f(2) + \\ & + (m^2 - \mathbf{p}_1 \cdot \mathbf{p}_2 - E_{\mathbf{p}_1} E_{\mathbf{p}_2}) \left[\frac{2E_+}{E_+^2 - \omega^2} \right] 2n_b(\omega) + \\ & \left. + 2 \frac{m^2 - \mathbf{p}_1 \cdot \mathbf{p}_2 - E_{\mathbf{p}_1} E_{\mathbf{p}_2}}{E_+ + \omega} \right\}, \quad (\text{A.8}) \end{aligned}$$

where we used the definitions given in Eqs. (11)–(14).

Finally, the expression in Eq. (10) is obtained from the result (A.8) by taking advantage of the symmetry of the integral in Eq. (A.2) to conveniently exchange $\mathbf{p}_1 \leftrightarrow \mathbf{p}_2$ in the terms $\sim N_f(2)$.

2. Renormalization

Let us now sketch the proof that the UV divergences present in the terms in Eq. (10) that are linear in the statistical distributions,

$$\begin{aligned} \mathbf{L}_f &\equiv -\beta V g^2 \int \frac{d^3 \mathbf{p}_1 d^3 \mathbf{p}_2}{(2\pi)^6} 4 \frac{1}{8\omega_{12} E_{\mathbf{p}_1} E_{\mathbf{p}_2}} \left[\bar{\mathcal{J}}_+(E_- + \omega_{12}) - \bar{\mathcal{J}}_-(E_+ - \omega_{12}) \right] N_f(1), \\ \mathbf{L}_b &\equiv \beta V g^2 \int \frac{d^3 \mathbf{p}_1 d^3 \mathbf{p}_2}{(2\pi)^6} 4 \frac{1}{8\omega_{12} E_{\mathbf{p}_1} E_{\mathbf{p}_2}} (-2) \bar{\mathcal{J}}_- E_+ n_b(\omega_{12}), \end{aligned} \quad (\text{A.9})$$

belong in fact to vacuum self-energy subdiagrams.

Using the auxiliary functions [37]

$$\mathcal{M}_f(p_1^4) \equiv \int_{-\infty}^{\infty} \frac{dp_2^4 dk^4}{(2\pi)^2} \frac{m^2 + P_1 \cdot P_2}{((p_2^4)^2 + E_{\mathbf{p}_2}^2)((k^4)^2 + \omega_{12}^2)} 2\pi \delta(k^4 - p_1^4 + p_2^4), \quad (\text{A.10})$$

$$\mathcal{M}_b(k^4) \equiv \int_{-\infty}^{\infty} \frac{dp_1^4 dp_2^4}{(2\pi)^2} \frac{m^2 + P_1 \cdot P_2}{((p_1^4)^2 + E_{\mathbf{p}_1}^2)((p_2^4)^2 + E_{\mathbf{p}_2}^2)} 2\pi \delta(k^4 - p_1^4 + p_2^4), \quad (\text{A.11})$$

where $P_i = (p_i^0, \mathbf{p}_i) = (ip_i^4, \mathbf{p}_i)$, which satisfy the identities:

$$\mathcal{M}_f(p_1^4) = \frac{1}{4E_{\mathbf{p}_2} \omega_{12}} \left\{ \frac{m^2 - \mathbf{p}_1 \cdot \mathbf{p}_2 - ip_1^4 E_{\mathbf{p}_2}}{ip_1^4 + E_{\mathbf{p}_2} + \omega_{12}} - \frac{m^2 - \mathbf{p}_1 \cdot \mathbf{p}_2 + ip_1^4 E_{\mathbf{p}_2}}{ip_1^4 - E_{\mathbf{p}_2} - \omega_{12}} \right\}, \quad (\text{A.12})$$

$$\mathcal{M}_b(k^4) = \frac{1}{4E_{\mathbf{p}_1} E_{\mathbf{p}_2}} (m^2 - \mathbf{p}_1 \cdot \mathbf{p}_2 - E_{\mathbf{p}_1} E_{\mathbf{p}_2}) \left[\frac{-2E_+}{E_+^2 - (ik^4)^2} \right], \quad (\text{A.13})$$

one can write:

$$\begin{aligned} \mathbf{L}_f &= -\beta V g^2 \int \frac{d^3 \mathbf{p}_1 d^3 \mathbf{p}_2 d^3 \mathbf{k}}{(2\pi)^6} \delta^{(3)}(\mathbf{k} - \mathbf{p}_1 + \mathbf{p}_2) 4 \frac{2N_f(1)}{2\omega} \mathcal{M}_f(-iE_{\mathbf{p}_1}), \\ \mathbf{L}_b &= -\beta V g^2 \int \frac{d^3 \mathbf{p}_1 d^3 \mathbf{p}_2 d^3 \mathbf{k}}{(2\pi)^6} \delta^{(3)}(\mathbf{k} - \mathbf{p}_1 + \mathbf{p}_2) 4 \frac{2n_b(\omega)}{2\omega} \mathcal{M}_b(-i\omega_{12}), \end{aligned} \quad (\text{A.14})$$

or, substituting the original expressions (A.10) and (A.11),

$$\begin{aligned} \mathbf{L}_f &= -\beta V g^2 \int \frac{d^3 \mathbf{p}_1}{(2\pi)^3} \frac{2N_f(1)}{2\omega} \left\{ \int \frac{d^3 \mathbf{p}_2 d^3 \mathbf{k}}{(2\pi)^6} \int_{-\infty}^{\infty} \frac{dp_2^4 dk^4}{(2\pi)^2} \times \right. \\ &\quad \left. \times (2\pi)^3 \delta^{(3)}(\mathbf{k} - \mathbf{p}_1 + \mathbf{p}_2) 2\pi \delta(k^4 - p_1^4 + p_2^4) \frac{4(m^2 + P_1 \cdot P_2)}{((p_2^4)^2 + E_{\mathbf{p}_2}^2)((k^4)^2 + \omega_{12}^2)} \right\} \Big|_{p_1^4 = -iE_{\mathbf{p}_1}}, \end{aligned} \quad (\text{A.15})$$

$$\begin{aligned} \mathbf{L}_b &= -\beta V g^2 \int \frac{d^3 \mathbf{k}}{(2\pi)^3} \frac{2n_b(\omega)}{2\omega} \left\{ \int \frac{d^3 \mathbf{p}_1 d^3 \mathbf{p}_2}{(2\pi)^6} \int_{-\infty}^{\infty} \frac{dp_1^4 dp_2^4}{(2\pi)^2} \times \right. \\ &\quad \left. \times (2\pi)^3 \delta^{(3)}(\mathbf{k} - \mathbf{p}_1 + \mathbf{p}_2) 2\pi \delta(k^4 - p_1^4 + p_2^4) \frac{4(m^2 + P_1 \cdot P_2)}{((p_1^4)^2 + E_{\mathbf{p}_1}^2)((p_2^4)^2 + E_{\mathbf{p}_2}^2)} \right\} \Big|_{k^4 = -i\omega_{12}}. \end{aligned} \quad (\text{A.16})$$

In Minkowski space, $P_i = (p_i^0 = ip_i^4, \mathbf{p}_i)$, $K = (k^0 = ik^4, \mathbf{k})$ and

$$\mathbf{L}_f = -\beta V g^2 \int \frac{d^3 \mathbf{p}_1}{(2\pi)^3} \frac{2N_f(1)}{2\omega} \left\{ \int \frac{d^4 P_2 d^4 K}{(2\pi)^4} (-i) \delta^{(4)}(K - P_1 + P_2) \frac{4(m^2 + P_1 \cdot P_2)}{(-P_2^2 + m^2)(-K^2 + m_\phi^2)} \right\} \Big|_{p_1^0 = E_{\mathbf{p}_1}} \quad (\text{A.17})$$

$$\mathbf{L}_b = -\beta V g^2 \int \frac{d^3 \mathbf{k}}{(2\pi)^3} \frac{2n_b(\omega)}{2\omega} \left\{ \int \frac{d^4 P_1 d^4 P_2}{(2\pi)^4} (-i) \delta^{(4)}(K - P_1 + P_2) \frac{4(m^2 + P_1 \cdot P_2)}{(-P_1^2 + m^2)(-P_2^2 + m^2)} \right\} \Bigg|_{k^0 = \omega_{12}} \quad (\text{A.18})$$

On the other hand, consider the one-loop diagrams contributing to the amputated bosonic and fermionic vacuum self-energies. When evaluated on the mass shell they satisfy:

$$\left(\text{Diagram 1} \right)_{\substack{vac \\ \text{amp} \\ m.s.}} = \left\{ g^2 \int \frac{d^4 P_2 d^4 K}{(2\pi)^8} (2\pi)^4 \delta^{(4)}(K - P_1 + P_2) \frac{2m^2 + 2P_1 \cdot P_2}{(P_2^2 - m^2)(K^2 - m_\phi^2)2m} \right\} \Bigg|_{\not{P}_1 = m} \quad (\text{A.19})$$

$$\left(\text{Diagram 2} \right)_{\substack{vac \\ \text{amp} \\ m.s.}} = \left\{ -g^2 N_F \int \frac{d^4 P_1 d^4 P_2}{(2\pi)^8} (2\pi)^4 \delta^{(4)}(K - P_1 + P_2) \frac{4(m^2 + P_1 \cdot P_2)}{(P_1^2 - m^2)(P_2^2 - m^2)} \right\} \Bigg|_{K^2 = m_\phi^2} \quad (\text{A.20})$$

Therefore, defining $P \equiv (i\omega_n^F + \mu, \mathbf{p}_1)$ and $Q \equiv (i\omega_l^B, \mathbf{k})$, we have:

$$T \sum_n \text{Tr} \left[\frac{1}{\not{P} - m} \right] = \frac{N_F(1) - 1}{2E_{\mathbf{p}_1}} 4m, \quad (\text{A.21})$$

$$T \sum_l \frac{1}{m_\phi^2 - Q^2} = \frac{2n_b(\omega) + 1}{2\omega}, \quad (\text{A.22})$$

so that

$$\not{\int}_P (-1) \text{Tr} \left[\frac{1}{\not{P} - m} \left(\text{Diagram 1} \right)_{\substack{vac \\ \text{amp} \\ m.s.}} \right] = -g^2 \int \frac{d^3 \mathbf{p}_1}{(2\pi)^3} \left[\frac{N_f(1) - 1}{2E_{\mathbf{p}_1}} \right] \left\{ \int \frac{d^4 P_2 d^4 K}{(2\pi)^4} \delta^{(4)}(K - P_1 + P_2) \times \right. \\ \left. \times \frac{4(m^2 + P_1 \cdot P_2)}{(P_2^2 - m^2)(K^2 - m_\phi^2)} \right\} \Bigg|_{\not{P}_1 = m}, \quad (\text{A.23})$$

$$\not{\int}_Q \frac{1}{m_\phi^2 - Q^2} \left(\text{Diagram 2} \right)_{\substack{vac \\ \text{amp} \\ m.s.}} = -g^2 N_F \int \frac{d^3 \mathbf{k}}{(2\pi)^3} \left[\frac{2n_b(\omega) + 1}{2\omega} \right] \left\{ \int \frac{d^4 P_1 d^4 P_2}{(2\pi)^4} \delta^{(4)}(K - P_1 + P_2) \times \right. \\ \left. \times \frac{4(m^2 + P_1 \cdot P_2)}{(P_1^2 - m^2)(P_2^2 - m^2)} \right\} \Bigg|_{K^2 = m_\phi^2}. \quad (\text{A.24})$$

Comparing Eqs. (A.23) and (A.24) with Eqs. (A.17) and (A.18), one concludes that \mathbf{L}_f and \mathbf{L}_b are written in terms of the vacuum self-energies as stated in Eqs. (15) and (16).

Thus the UV renormalization of these terms results directly from adopting renormalized expressions for these self-energies. Using dimensional regularization in the $\overline{\text{MS}}$ scheme, the measure in momentum integrals is modified as

$$\int \frac{d^d P}{(2\pi)^d} \mapsto \left(\frac{e^\gamma \Lambda^2}{4\pi} \right)^{\epsilon/2} \int \frac{d^d P}{(2\pi)^d}, \quad (\text{A.25})$$

where $\epsilon = 4 - d$, with d being the space-time dimension, Λ the renormalization scale and γ the Euler constant. A standard computation yields for the amputated vacuum one-loop self-energies evaluated on the mass shell the following regularized expressions:

$$\left(\text{Diagram 1} \right)_{\substack{vac \\ \text{amp} \\ m.s.}} = -\frac{g^2}{(4\pi)^2} \int_0^1 dx [m(1+x)] \left[\frac{2}{\epsilon} + \log \left(\frac{\Lambda^2}{\Delta_f} \right) + O(\epsilon) \right], \quad (\text{A.26})$$

$$\left(\text{diagram} \right)_{\substack{\text{vac} \\ \text{amp} \\ \text{m.s.}}} = \frac{g^2}{(4\pi)^2} N_F \int_0^1 dx \Delta_b \left[\frac{24}{\epsilon} + 4 + 12 \log \left(\frac{\Lambda^2}{\Delta_b} \right) + O(\epsilon) \right], \quad (\text{A.27})$$

where

$$\Delta_f \equiv \{m^2(1-x) + m_\phi^2 x - x(1-x)P_1^2\}|_{p_1=m} = m^2(1-x)^2 + m_\phi^2 x, \quad (\text{A.28})$$

$$\Delta_b \equiv \{m^2 - x(1-x)K^2\}|_{K^2=m_\phi^2} = m^2 - x(1-x)m_\phi^2. \quad (\text{A.29})$$

Defining the integrals over the Feynman parameter x as

$$\alpha_1 \equiv \int_0^1 dx (1+x) \log \left(\frac{\Lambda^2}{\Delta_f} \right), \quad (\text{A.30})$$

$$\alpha_2 \equiv \int_0^1 dx \Delta_b, \quad (\text{A.31})$$

$$\alpha_3 \equiv \int_0^1 dx \Delta_b \log \left(\frac{\Lambda^2}{\Delta_b} \right), \quad (\text{A.32})$$

and substituting the renormalized expressions, obtained from Eqs. (A.26) and (A.27) by subtracting the poles in $\epsilon = 0$, in Eqs. (15) and (16), one arrives at the final results in Eqs. (17) and (18). The solution of the integrals α_i is straightforward, yielding Eqs. (19)–(21).

C. The integral J_1

Finally, in order to obtain the final analytical result in Eqs. (24)–(31), the integral in Eq. (23) must be calculated. Explicitly, we have:

$$J_1 = \int \frac{d^3 \mathbf{p}_1 d^3 \mathbf{p}_2}{(2\pi)^6} \frac{\theta(\mu - E_1)\theta(\mu - E_2)}{2E_1 E_2} \left\{ \frac{4m^2 - m_\phi^2}{(E_1 - E_2)^2 - |\mathbf{p}_1 - \mathbf{p}_2|^2 - m_\phi^2} - 1 \right\}, \quad (\text{33})$$

$$\equiv \frac{1}{(2\pi)^4} [j_I - 2j_{II}], \quad (\text{34})$$

where we used the expression for $\overline{\mathcal{J}}_+$ given in Eq. (11) and defined:

$$j_I \equiv \int \frac{d^3 \mathbf{p}_1 d^3 \mathbf{p}_2}{(2\pi)^2} \frac{\theta(\mu - E_1)\theta(\mu - E_2)}{2E_1 E_2} \frac{4m^2 - m_\phi^2}{(E_1 - E_2)^2 - |\mathbf{p}_1 - \mathbf{p}_2|^2 - m_\phi^2}, \quad (\text{35})$$

$$j_{II} \equiv \frac{1}{2} \int \frac{d^3 \mathbf{p}_1 d^3 \mathbf{p}_2}{(2\pi)^4} \frac{\theta(\mu - E_1)\theta(\mu - E_2)}{2E_1 E_2}. \quad (\text{36})$$

After evaluating the angular integration, one obtains:

$$j_I = \frac{4m^2 - m_\phi^2}{2} \int_m^\mu dE_1 dE_2 \log \left[\frac{2m^2 - m_\phi^2 - 2E_1 E_2 + 2p_1 p_2}{2m^2 - m_\phi^2 - 2E_1 E_2 - 2p_1 p_2} \right] \equiv \frac{4m^2 - m_\phi^2}{2} \mathcal{I}_I,$$

$$j_{II} = \int_m^\mu dE_1 dE_2 p_1 p_2 \equiv (\mathcal{I}_{II})^2, \quad (\text{37})$$

where $p_i \equiv \sqrt{E_i^2 - m^2}$.

The integral \mathcal{I}_{II} is simple, yielding:

$$\mathcal{I}_{II} = \frac{1}{2} \left\{ \mu p_f - m^2 \log \left[\frac{\mu + p_f}{m} \right] \right\} \equiv \frac{u}{2}. \quad (\text{38})$$

On the other hand, the integral \mathcal{I}_I is extremely more involved. One of the difficulties is the fact that it corresponds to a double integral of a *log* whose argument contains roots which depend on the variable of integration. It is possible,

through a convenient transformation of variables, to obtain an integrand without roots. A change of variables with this feature was presented in Ref. [24]:

$$E_i \mapsto x_i = \frac{p_i}{E_i + m} \Rightarrow \quad (39)$$

$$p_i = \frac{2mx_i}{1-x_i^2}; \quad E_i = m \frac{1+x_i^2}{1-x_i^2}; \quad dE_i = \frac{4mx_i}{(1-x_i^2)^2} dx_i. \quad (40)$$

Once this new set of variables is adopted, the procedure to solve the integral \mathcal{I}_I includes a sequence of partial integrations and several algebraic manipulations until an expression is reached such that it contains only analytically solvable integrals, at least for a software of algebraic computation. Solving these integrals, one arrives at:

$$\begin{aligned} \mathcal{I}_I = & p_f^2 - 2m^2 \bar{\mathcal{K}}_{\log} \left(\frac{p_f}{\mu + m}, \frac{m_\phi^2}{4m^2} \right) + \mu^2 \frac{m_\phi^2}{2m^2} \log \left[\frac{m_\phi^2}{4p_f^2 + m_\phi^2} \right] + \\ & + \left(1 - \frac{m_\phi^2}{2m^2} \right) \left\{ 2\mu p_f - m^2 \log \left[\frac{\mu + p_f}{m} \right] \right\} \log \left[\frac{m}{\mu + p_f} \right] + \\ & + \frac{2m_\phi}{m} \sqrt{1 - \frac{m_\phi^2}{4m^2}} \left\{ \mu p_f - \frac{m^2}{2} \log \left(\frac{\mu + p_f}{m} \right) \right\} \left\{ \tan^{-1} \left(\frac{-p_f m_\phi}{2m(\mu + m) \sqrt{1 - \frac{m_\phi^2}{4m^2}}} \right) + \right. \\ & \left. + \tan^{-1} \left(\frac{p_f}{m_\phi \sqrt{1 - \frac{m_\phi^2}{4m^2}}} \left[2 - \frac{m_\phi^2}{2m(\mu + m)} \right] \right) \right\}, \end{aligned} \quad (41)$$

where $\bar{\mathcal{K}}_{\log}$ is the last integration still to be done:

$$\bar{\mathcal{K}}_{\log}(\bar{x}, z) = \sum_{\pm} \sqrt{z(1-z)} \int_0^{\bar{x}} dx \log \left(\frac{1-x}{1+x} \right) \frac{d}{dx} \left\{ \tan^{-1} \left[\frac{\frac{\bar{x} \pm x}{1-x^2} - \bar{x} z}{\sqrt{z(1-z)}} \right] \right\}. \quad (42)$$

The solution of $\bar{\mathcal{K}}_{\log}$ can be written in terms of products of logarithms whose arguments can assume negative values, resulting in a complex result in general. These imaginary parts must cancel out in the end. To verify this cancellation and simplify the expression, it is convenient to consider two complementary regimes: $z = m_\phi^2/4m^2 > 1$ and $z = m_\phi^2/4m^2 < 1$, and to use the fact that $\bar{x} = p_f/(\mu + m) < 1$. The final result, after a very long set of manipulations, is the one given in Eqs. (24)–(31).

-
- [1] T. Baier, E. Bick and C. Wetterich, Phys. Rev. B **62**, 15471 (2000); **70**, 125111 (2004); Phys. Lett. B **605**, 144 (2005).
[2] N. K. Glendenning, *Compact Stars — Nuclear Physics, Particle Physics, and General Relativity* (Springer, New York, 2000); H. Heiselberg and M. Hjorth-Jensen, Phys. Rept. **328**, 237 (2000);
[3] M. A. Stephanov, PoS **LAT2006**, 024 (2006).
[4] M. G. Alford, K. Rajagopal, T. Schaefer and A. Schmitt, arXiv:0709.4635 [hep-ph].
[5] E. Laermann and O. Philipsen, Ann. Rev. Nucl. Part. Sci. **53**, 163 (2003).
[6] E. S. Fraga, R. D. Pisarski and J. Schaffner-Bielich, Phys. Rev. D **63**, 121702 (2001); Nucl. Phys. A **702**, 217 (2002).
[7] J. P. Blaizot, E. Iancu and A. Rebhan, Phys. Rev. D **63**, 065003 (2001).
[8] J. O. Andersen and M. Strickland, Phys. Rev. D **66**, 105001 (2002).
[9] E. Braaten, Nucl. Phys. A **702**, 13 (2002).
[10] I. H. Lee, J. Shigemitsu and R. E. Shrock, Nucl. Phys. B **330**, 225 (1990).
[11] P. Gerhold and K. Jansen, JHEP **0709**, 041 (2007); **0710**, 001 (2007).
[12] An interesting example is given by the study of the phase diagram of the Gross-Neveu model using the method of optimized perturbation theory (OPT), as done in Refs. J. L. Kneur, M. B. Pinto and R. O. Ramos, Phys. Rev. D **74**, 125020 (2006); J. L. Kneur, M. B. Pinto, R. O. Ramos and E. Staudt, Phys. Lett. B **657**, 136 (2007); Phys. Rev. D **76**, 045020 (2007).
[13] This approach is particularly useful in the case of the chiral and deconfinement transitions in QCD, where one can use lattice data to fix parameters of an effective field theory as done, for instance, in Refs: A. Dumitru and R. D. Pisarski, Phys. Lett. B **504**, 282 (2001); O. Scavenius, A. Dumitru and J. T. Lenaghan, Phys. Rev. C **66**, 034903 (2002); E. Fraga and A. Mocsy, Braz. J. Phys. **37**, 281 (2007).
[14] L. F. Palhares and E. S. Fraga, Braz. J. Phys. **37**, 26 (2007); E. S. Fraga and L. F. Palhares, AIP Conf. Proc. **892**, 479 (2007).

- [15] L. F. Palhares and E. S. Fraga, *Int. J. Mod. Phys. E* **16**, 2806 (2007).
- [16] A. Taurines, *private communication*.
- [17] Up to two loop order, the diagrams with self-interaction vertices are either one-particle reducible or independent of the fermionic chemical potential μ .
- [18] L. F. Palhares and E. S. Fraga, to appear.
- [19] J. I. Kapusta and C. Gale, *Finite-Temperature Field Theory: Principles and Applications* (Cambridge University Press, 2006).
- [20] Since we are concerned only with the zero-temperature limit, there are no odd powers of g coming from resummed contributions of the zero Matsubara mode for bosons in the perturbative series. Even including hard dense loop corrections, they would only modify the $g^{2\ell}$ terms [8]. Here we deliberately do not include resummation corrections, keeping the focus on the analytic computation of the thermodynamic potential for *arbitrary* fermion and scalar masses, including the RG flow of coupling and masses.
- [21] R. J. Furnstahl, R. J. Perry and B. D. Serot, *Phys. Rev. C* **40**, 321 (1989).
- [22] I. A. Akhiezer e S. V. Peletminski, *ZhETF (USSR)* **38**, 1829 (1960) [*JETP(Sov. Phys.)* **11**, 1316 (1960)].
- [23] B. A. Freedman e L. D. McLerran, *Phys. Rev. D* **16**, 1147 (1977).
- [24] T. Toimela, *Int. J. Theor. Phys.* **24**, 901 (1985) [Erratum-ibid. **26**, 1021 (1987)].
- [25] E. Farhi and R. L. Jaffe, *Phys. Rev. D* **30**, 2379 (1984).
- [26] J. I. Kapusta, *Nucl. Phys. B* **148**, 461 (1979).
- [27] B. A. Freedman e L. D. McLerran, *Phys. Rev. D* **16**, 1169 (1977).
- [28] V. Baluni, *Phys. Rev. D* **17**, 2092 (1978).
- [29] E. S. Fraga e P. Romatschke, *Phys. Rev. D* **71**, 105014 (2005).
- [30] M. Abramowitz and I. A. Stegun (eds.), *Handbook of Mathematical Functions* (Dover, New York, 1965).
- [31] A. Grozin, *Lectures on QED and QCD: practical calculation and renormalization of one- and multi-loop Feynman diagrams* (World Scientific, 2007).
- [32] As discussed in Ref. [33], the difference between the full thermodynamic potential and the vacuum one satisfies a Callan-Symanzik equation with zero anomalous dimension. Therefore, the exact expression for the thermodynamic potential normalized to zero in the vacuum is RG invariant. However, within the perturbative approach, the truncation of the series at any finite order spoils this invariance, rendering Ω_Y sensitive to the renormalization scale Λ . Besides the physically grounded choice of the scale Λ through the phenomenological knowledge of the features of a given system, another possible criterium is to minimize the sensitivity of Ω_Y with respect to this renormalization scale. In this latter vein, one can rewrite Ω_Y in Eq. (22) in such a way that the explicit dependence on Λ , of the form $\sim \alpha_Y \log(\Lambda)$, is absorbed in the running of α_Y .
- [33] B. A. Freedman and L. D. McLerran, *Phys. Rev. D* **16**, 1130 (1977).
- [34] S. R. Coleman and D. J. Gross, *Phys. Rev. Lett.* **31**, 851 (1973).
- [35] D. J. Gross and A. Neveu, *Phys. Rev. D* **10**, 3235 (1974).
- [36] S. Hands, *Prog. Theor. Phys. Suppl.* **168**, 253 (2007).
- [37] The basic idea of this manipulation is to use the integral representation of the Dirac delta function to factor the integrations and solve them independently, as described in [38].
- [38] P. Romatschke, *Thermal corrections to the sunset diagram, Diplomarbeit* (Technische Universität Wien, 2001).